Control of the Geometric Phase and Nonequivalence between Geometric-Phase Definitions in the Adiabatic Limit

Xiaosong Zhu,[1,2,3] Peixiang Lu,[2,3,*] and Manfred Lein[1,†]
[1]Leibniz University Hannover, Institute of Theoretical Physics, 30167 Hannover, Germany
[2]Wuhan National Laboratory for Optoelectronics and School of Physics, Huazhong University of Science and Technology, Wuhan 430074, China
[3]Optics Valley Laboratory, Hubei 430074, China

(Received 30 September 2019; accepted 18 November 2021; published 20 January 2022)

If the time evolution of a quantum state leads back to the initial state, a geometric phase is accumulated that is known as the Berry phase for adiabatic evolution or as the Aharonov-Anandan (AA) phase for nonadiabatic evolution. We evaluate these geometric phases using Floquet theory for systems in time-dependent external fields with a focus on paths leading through a degeneracy of the eigenenergies. Contrary to expectations, the low-frequency limits of the two phases do not always coincide. This happens as the degeneracy leads to a slow convergence of the quantum states to adiabaticity, resulting in a nonzero finite or divergent contribution to the AA phase. Steering the system adiabatically through a degeneracy provides control over the geometric phase as it can cause a π shift of the Berry phase. On the other hand, we revisit an example of degeneracy crossing proposed by AA. We find that, at suitable driving frequencies, both geometric-phase definitions give the same result and the dynamical phase is zero due to the symmetry of time evolution about the point of degeneracy, providing an advantageous setup for manipulation of quantum states.

DOI: 10.1103/PhysRevLett.128.030401

When a quantum-mechanical system undergoes a closed circuit in parameter space, an adiabatically evolving state may acquire a geometric phase, known as the Berry phase [1], in addition to its dynamical phase, where the latter is essentially the time-integrated energy. The geometric phase is an important fundamental concept and it appears in many fields including molecular physics [2–4], solid-state physics [5–8], ultracold atoms [9,10], optics [11–15], and quantum computation [16–18]. Following Berry, the geometric phase can be evaluated from the instantaneous eigenstates by integration of the Berry connection, without reference to time evolution. However, since the adiabatic approximation is not necessarily valid [19,20], one may resort to a nonadiabatic generalization suggested by Aharonov and Anandan (AA) [21,22]. To calculate the geometric phase, both Berry and AA consider the total phase acquired during the cyclic evolution and they subtract the dynamical phase, but they apply different definitions of the latter: Berry uses the time-integrated instantaneous eigenenergy whereas AA use the time-integrated energy expectation value. It is generally believed that the two geometric phases agree in the adiabatic limit for unitary evolution [21,22], but we show a counterexample below.

The vast majority of existing studies exclude circuits leading through a degeneracy (crossing or touching of the energy levels). It is worth asking what effects and applications will emerge in such a case. One example, a spin-1/2 particle driven by a slowly varying periodic magnetic field that passes through zero, was suggested by AA [21]. Without rigorous calculation, they argued that the system remains in an energy eigenstate (i.e., it behaves adiabatically in our terminology) and that the AA phase has a well-defined limit. Our analysis confirms both statements, which is important for quantum-state manipulation, but as we demonstrate, the second statement does not necessarily hold in other examples involving a degeneracy.

First, we investigate a Ne^+ ion driven by periodic laser fields, comparing two types of driving protocols: either enclosing a degeneracy or passing through it. We consider laser fields because their time-dependent electric-field vector follows a closed curve in the plane of polarization, i.e., a circuit in parameter space. A circularly polarized (CP) single-color field creates a circuit encircling the degeneracy. Using additional colors allows for more complex paths. We employ bicircular fields, i.e., combining two circular fields of different colors, which have recently been used for fundamental studies and novel applications [23–32]. With equal strengths of both colors, the field crosses zero several times per cycle. Therefore, such a 1 : 1 field steers the system through a degeneracy if the energy eigenstates are degenerate at zero field strength. We demonstrate both analytically and numerically, by introducing a numerical measure termed *adiabaticity indicator*, that the evolution can be adiabatic despite the degeneracy. However, we find a breakdown of the equivalence between the AA phase and Berry phase in the adiabatic limit. We also show that the passage through the degeneracy causes a controlled π shift of the Berry phase. In the end, we revisit AA's spin-1/2 example, finding that,

due to a symmetry of time evolution, the AA phase for suitably chosen states is the same as the adiabatic Berry phase, even in the nonadiabatic regime.

Floquet theory and geometric phase.—A systematic way [33–35] to obtain the AA phase [36] follows from Floquet theory, the tool to describe periodically driven quantum matter [37–43]. According to the Floquet theorem, the time-dependent Schrödinger equation (TDSE) $\mathrm{i}\partial/\partial t|\Psi(t)\rangle = H(t)|\Psi(t)\rangle$ with periodic Hamiltonian $H(t) = H(t+T)$ has solutions $|\Psi(t)\rangle = e^{-i\mathcal{E}_F t}|P(t)\rangle$ with quasienergies $\mathcal{E}_F$ and time-periodic states $|P(t+T)\rangle = |P(t)\rangle$ satisfying the Floquet equation $(H - i\partial/\partial t)|P(t)\rangle = \mathcal{E}_F|P(t)\rangle$ [44]. These solutions return *exactly* to the initial state, up to an overall phase determined by the quasienergy: The total phase accumulation in one period is $-\mathcal{E}_F T$. Subtracting the dynamical phase $-\bar{H}T$ based on the time-averaged energy expectation value $\bar{H} = \int_0^T \langle\Psi(t)|H(t)|\Psi(t)\rangle dt/T$, we obtain the AA phase $\gamma_A = (\bar{H} - \mathcal{E}_F)T$. For practical calculations, the periodic state $|P(t)\rangle$ is Fourier expanded as $|P(t)\rangle = \sum_n e^{-in\omega t}|F_n\rangle$ with $\omega = 2\pi/T$ so that the Floquet states are determined by a matrix eigenvalue equation [37,38]. The AA phase takes the form $\gamma_A = 2\pi\bar{n}$ with $\bar{n} = \sum_n \langle F_n|F_n\rangle n$, see also Refs. [34,45]. We interpret this result using the photon-channel perspective [24,46]: $\langle F_n|F_n\rangle$ is the weight of the contribution to the Floquet state reached by absorption of the photon energy $n\omega$. Hence the AA phase is a measure of the population redistribution by photon absorption or emission.

An alternative view on geometric phases is provided by low-frequency Floquet theory, where the quasienergy is expanded as $\mathcal{E}_F = \bar{\mathcal{E}} + \omega\mathcal{E}_F^{(1)} + \cdots$ [45,47–52] with $\bar{\mathcal{E}} = \int_0^T \mathcal{E}(t)dt/T$. Here, $\mathcal{E}(t)$ is an eigenvalue of $H(t)$. Using the dynamical phase $-\bar{\mathcal{E}}T$ as in Ref. [1], we introduce a nonadiabatic Berry phase $\gamma_B = (\bar{\mathcal{E}} - \mathcal{E}_F)T$ that includes nonadiabaticity via $\mathcal{E}_F(\omega)$. The common adiabatic Berry phase is then equal to the low-frequency limit $\gamma_B^{(0)} = \lim_{\omega\to 0}\gamma_B = -2\pi\mathcal{E}_F^{(1)}$. It is observable by measuring the quasienergy, for example, from positions of peaks in electron spectra from light-induced ionization [43,53]. Note that the low-frequency limit of the AA phase can be written as $\lim_{\omega\to 0} i\int_0^{2\pi/\omega}\langle P(t)|\partial_t|P(t)\rangle dt$, which becomes the adiabatic Berry phase only when replacing the state $|P(t)\rangle$ by its low-frequency limit before carrying out the integration, i.e., by a possibly illicit rearrangement of limits.

Adiabaticity of time evolution.—We term an evolution adiabatic if the state $|\Psi(t)\rangle$ always remains close to an instantaneous eigenstate $|j(t)\rangle$ of the Hamiltonian $H(t)$, i.e., the time-dependent fidelity $\mathcal{F}_j(t) = |\langle j(t)|\Psi(t)\rangle|^2$ satisfies $\min_t \mathcal{F}_j(t) \approx 1$. To quantify the adiabaticity of any numerical wave function, we introduce the adiabaticity indicator $\mathcal{F} = \max_j \min_t \mathcal{F}_j(t)$, where the maximum over j selects the closest eigenstate. Values $\mathcal{F} \approx 1$ indicate that $|\Psi(t)\rangle$ is always close to this eigenstate.

In the following, we discuss adiabatic motion with passages through degeneracies, cf. Ref. [54]. The evolving state is expanded as $|\Psi(t)\rangle = \sum_l a_l(t)e^{-i\int_0^t \mathcal{E}_l(\tau)d\tau}|l(t)\rangle$ with eigenstates $|l\rangle$ chosen such that $\langle l|\dot{l}\rangle = 0$ and energy eigenvalues $\mathcal{E}_l$. The evolution is adiabatic if the change of the coefficient a_m,

$$\Delta a_m(t) = -\sum_{l\neq m}\int_0^t a_l(\tau)\langle m|\dot{l}\rangle e^{if(\tau)}d\tau, \tag{1}$$

remains small [55,56], where $f(\tau) = \int_0^\tau \mathcal{E}_{ml}(\tau')d\tau'$ and $\mathcal{E}_{ml} = \mathcal{E}_m - \mathcal{E}_l$. The exponential oscillates rapidly except near the saddle points t_0 satisfying $f'(t_0) = \mathcal{E}_{ml}(t_0) = 0$ [57,58]. These are the instants when the system crosses the degeneracy. The prefactor $a_l(\tau)\langle m|\dot{l}\rangle$ varies slowly compared to the exponential. It is therefore treated as constant. The integral is dominated by the regions around the saddle points, so we expand $f(\tau) = f(t_0) + f'(t_0)(\tau - t_0) + \cdots$. Close to t_0, we also exploit $\mathcal{E}_{ml}(t) \propto [\omega(t-t_0)]^N$ with positive integer N. (In the examples below, we have $N = 2$ in Ne^+ due to the quadratic Stark shift and $N = 1$ for the spin-1/2 particle.) Hence, the first nonzero derivative of f is $f^{(N+1)}(t_0) \propto \omega^N$. Keeping the two lowest contributing orders, we have $f(\tau) = f(t_0) + \alpha\omega^N(\tau - t_0)^{N+1}$ with a constant α. Substituting $s = (\tau - t_0)\omega^{N/(N+1)}$, the contribution of one saddle point to the integral in Eq. (1) is

$$a_l(t_0)\langle m|\dot{l}\rangle e^{if(t_0)}\int_{-\infty}^{\infty} e^{i\alpha s^{N+1}}\omega^{-\frac{N}{N+1}}ds \propto \omega^{\frac{1}{N+1}}, \tag{2}$$

where $\langle m|\dot{l}\rangle \propto \omega$ is used. Thus, at $\omega \to 0$, we find $\Delta a_m \to 0$ and the evolution converges to adiabaticity despite the passage through the degeneracy and irrespective of the value of N. However, our analysis indicates that adiabaticity is approached slower for larger N.

Thus, for Floquet states passing through degeneracies, the nonadiabatic admixture $|\Psi_{\mathrm{na}}(t)\rangle$ to the eigenstate with eigenvalue $\mathcal{E}$ behaves as $\langle\Psi_{\mathrm{na}}(t)|\Psi_{\mathrm{na}}(t)\rangle \propto \omega^{2/(N+1)}$ if we ignore any additional substructure due to multiphoton resonances. This leads to $\bar{H} - \bar{\mathcal{E}} \propto \omega^{2/(N+1)}$. Together with $\mathcal{E}_F = \bar{\mathcal{E}} + \omega\mathcal{E}_F^{(1)} + \cdots$ and $\gamma_A = (\bar{H} - \mathcal{E}_F)2\pi\omega^{-1}$, we find $\gamma_A - \gamma_B^{(0)} \propto \omega^{-1+[2/(N+1)]}$. The striking conclusion is that the AA phase differs from the Berry phase in the adiabatic limit. It diverges at $\omega \to 0$ for $N \geq 2$.

Ne^+ *ion in a light field.*—This set of examples is motivated by the experimental feasibility of preparing rare-gas ions in one of their degenerate ring-current states [59,60] and by the possibility to lift this degeneracy by an external field. We treat a single active electron in an effective potential [61] and we restrict the analysis to the $2p_\pm$ states with magnetic quantum numbers ± 1 and the $2s$ state [62–64]. The bicircular electric field composed of frequencies ω and 2ω is [31]

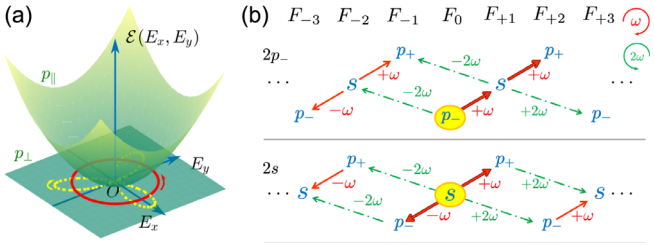

FIG. 1. (a) Energy surfaces of the $2p$ states for Ne^+ in an electric field and paths of the electric field in the parameter space for CP (red) and 1:1 bicircular (yellow) fields. (b) Illustration of the possible transitions in the bicircular field.

$$\mathbf{E}(t) = E_1[\cos(\omega t)\hat{\mathbf{e}}_x + \sin(\omega t)\hat{\mathbf{e}}_y] + E_2[\cos(2\omega t)\hat{\mathbf{e}}_x - \sin(2\omega t)\hat{\mathbf{e}}_y]. \quad (3)$$

A single-color CP field is a special case with $E_2 = 0$. The time-dependent Hamiltonian reads $H(t) = H_0 + \mathbf{r}\cdot\mathbf{E}(t)$. In one optical cycle, the field follows a closed circuit in the parameter space given by the E_x-E_y-plane, see Fig. 1(a), which shows also the adiabatic eigenenergies for the $2p$ states as a function of the field. One of the orbitals tends to spatially align along the field (labeled $p_\parallel$), exhibiting a parabolic energy surface, whereas the other one tends to align perpendicularly (labeled $p_\perp$) with flat energy surface [62]. The degeneracy at $\mathbf{E} = 0$ is reminiscent of a Renner-Teller level touching, which shows no adiabatic Berry phase when encircled by an adiabatic path [65]. In the Floquet calculation, we expand $|F_n\rangle = \sum_j c_{nj}|\phi_j\rangle$, where $|\phi_j\rangle$ are the field-free states ($j = p_-, s, p_+$). Field-induced transitions obey angular-momentum conservation rules. The possible photon channels from $2p_-$ and $2s$ as initial states are illustrated in Fig. 1(b). A CP field permits only few channels, indicated by the thick arrows.

We first consider a CP driving field. The numerically calculated AA phases γ_A for the Floquet states are presented in Fig. 2(a) as a function of the dimensionless parameter $\mathcal{N} = 2D^2E_0^2/(\omega\Delta\mathcal{E})$, where $E_0^2 = E_1^2 + E_2^2$, $\Delta\mathcal{E} = 0.8509$ a.u. is the gap between the field-free $2p$ and $2s$ energies, and $D = \langle\phi_{p_\pm}|x|\phi_s\rangle = -0.3513$ a.u. is the transition dipole. The AA phases for the two $2p$ states have opposite signs and vary continuously from zero at small $\mathcal{N}$ to $\pm 2\pi$ at $\mathcal{N} \to \infty$ [66]. It is intuitive that γ_A vanishes at large frequencies as there is no time ($T \to 0$) to accumulate phase. To understand the low-frequency limit, we plot the adiabaticity indicator $\mathcal{F}$ for p-type states in Fig. 2(a). It quantifies the similarity of the Floquet state to the instantaneous energy eigenstates,

$$|p_\parallel(t)\rangle \propto \left(e^{2i\omega t}, \frac{e^{i\omega t}(\sqrt{\Delta\mathcal{E}^2 + 8D^2E_0^2} - \Delta\mathcal{E})}{2DE_0}, 1\right)^{\mathsf{T}} \quad (4)$$

and $|p_\perp(t)\rangle \propto (-e^{2i\omega t}, 0, 1)^{\mathsf{T}}$, where the three components refer to the basis given by the field-free states p_-, s, p_+. The adiabaticity indicator converges to 1 at low frequency ($\mathcal{N} \to \infty$), indicating that the evolution becomes adiabatic. Next, we derive the value of the AA phase assuming $\mathcal{F} = 1$. From Eq. (4), we see $|\langle\phi_{p_-}|p_\parallel\rangle|^2 = |\langle\phi_{p_+}|p_\parallel\rangle|^2 = (1 - |\langle\phi_s|p_\parallel\rangle|^2)/2$. Hence, when the field-free p_- state is turned into the state $|p_\parallel\rangle$ by the presence of the external field [see upper panel of Fig. 1(b)], the mean number of absorbed quanta ω for the transitions to s and p_+ is $\bar{n} = 1$. Inserting into $\gamma_A = 2\pi\bar{n}$ gives $\gamma_A = 2\pi$, in agreement with the numerical finding at low frequency. In analogy, one finds -2π for the other p-type state. At intermediate $\mathcal{N}$, the system deviates from adiabaticity, resulting in nontrivial values of γ_A. For the $2s$ state, the transitions from s to $p_\pm$ via absorbing or emitting photons are symmetric, so that $\bar{n} = 0$ and $\gamma_A = 0$. Apparently, symmetry breaking of the photon channels for the ring-current initial states causes nonzero geometric phases. A similar conclusion drawn for pseudorotating molecules [67] was that the nuclear ring currents allowed by a degeneracy play a role in the nonzero geometric phase. The CP field [red curve in Fig. 1(a)] drives the system around the degeneracy. With this driving, the adiabatic limit of the AA phase equals the adiabatic Berry phase obtained by integrating the Berry connection.

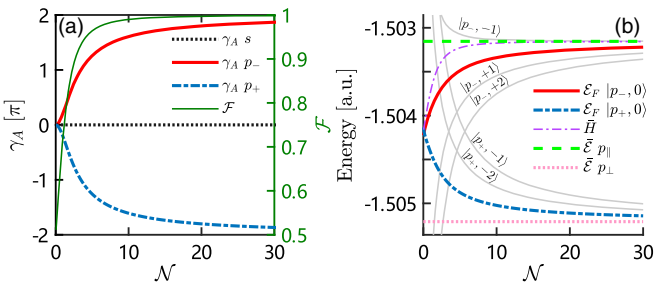

FIG. 2. Results for a CP field with intensity 5×10^{14} W/cm^2. (a) AA phases γ_A and adiabaticity indicator $\mathcal{F}$ for p-type states. (b) Energy curves. $|p_-, 0\rangle$ denotes a solution for $|P(t)\rangle$ that resembles the p_- state at the smallest considered $\mathcal{N}$, while $|p_-, n\rangle$ denotes a solution with quasienergy differing by $-n\omega$.

As Fig. 2(b) shows, the quasienergies $\mathcal{E}_F$ of the p states converge to the time-averaged instantaneous eigenenergy $\bar{\mathcal{E}}$ at $\mathcal{N} \to \infty$. A fit of the asymptotic behavior reveals that $\bar{\mathcal{E}} - \mathcal{E}_F \propto \omega^2 \pmod{\omega}$. This means that the Berry phase $\gamma_B = (\bar{\mathcal{E}} - \mathcal{E}_F)T$ vanishes in the low-frequency limit (up to integer multiples of 2π). Similarly, $\bar{H} - \mathcal{E}_F$ behaves as $\omega^2 \pmod{\omega}$, implying that the AA phase approaches zero (mod 2π).

A bicircular field permits more photon channels [Fig. 1(b)] and multiphoton resonances appear. Figure 3 shows results for $E_1 : E_2 = 1:1$. Three times per cycle, this bicircular field [yellow curve in Fig. 1(a)] passes through zero and thus drives the system through the degeneracy. The adiabaticity indicator $\mathcal{F}$ in Fig. 3(a) shows sharp drops at the multiphoton resonances, implying highly nonadiabatic evolution. Nevertheless, at off-resonance low frequencies, $\mathcal{F}$ approaches unity. For one such case,

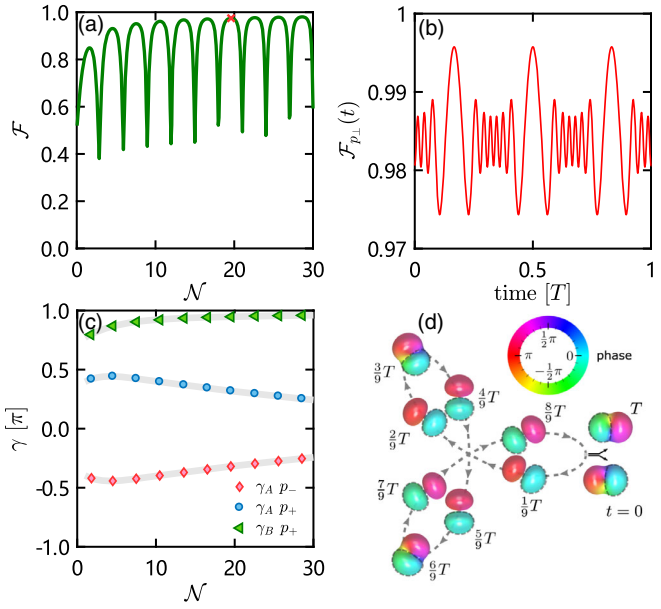

FIG. 3. Results for a 1:1 bicircular field with total intensity 5×10^{14} W/cm^2. (a) Adiabaticity indicator for p-type states. (b) Time-dependent fidelity $\mathcal{F}_{p_\perp}(t) = |\langle p_\perp(t)|\Psi(t)\rangle|^2$ for $\mathcal{N} = 19.6$ (see red cross in (a)). (c) AA phase γ_A and Berry phase γ_B of p states at off-resonance frequencies. Gray curves serve as a guide to the eye. (d) Evolution of the $p_\parallel$-like Floquet orbital at $\mathcal{N} = 1.7$. The colors represent the position-dependent phase after subtracting the dynamical phase $-\int_0^t \mathcal{E}(\tau)d\tau$. The change of this phase over one period gives the Berry phase γ_B.

the time-dependent fidelity is shown in Fig. 3(b). It stays close to unity despite noticeable oscillations.

In the following, we focus on the off-resonance geometric phases of p states. (Those for the s state are zero). We choose representative off-resonance points and plot the corresponding phases γ_A and γ_B, shifted by integer multiples of 2π into the interval $[-\pi, \pi]$, see Fig. 3(c). Here, the astounding anomalous behavior expected from the passage through the degeneracy is found. Unlike the result in Fig. 2(a), the AA phase does not have an adiabatic limit, although the time evolution becomes adiabatic.

Integration of the Berry connection for the instantaneous eigenstate $|p_\perp(t)\rangle \propto (-e^{-i\omega t}, 0, 1)^\mathsf{T}$ yields π (mod 2π), in agreement with γ_B tending to π in Fig. 3(c). Fitting the asymptotic behavior of the energies at $\omega \to 0$ yields $\bar{\mathcal{E}} - \mathcal{E}_F \approx 0.5\omega$ and it confirms the analytical expectation $\bar{H} - \mathcal{E}_F \propto \omega^{2/3}$. Indeed, both energy differences converge to zero, but with different speeds. When computing the geometric phases as $\gamma_A = (\bar{H} - \mathcal{E}_F)T$ and $\gamma_B = (\bar{\mathcal{E}} - \mathcal{E}_F)T$, the energies are multiplied with a diverging factor $T = 2\pi/\omega \to \infty$. Thus, γ_B converges to the finite value π, while $|\bar{H} - \mathcal{E}_F|$ does not decrease fast enough to let γ_A converge. γ_A scales as $\omega^{-1/3}$ as expected.

A bicircular field with $E_1 : E_2 \neq 1:1$ creates multiphoton resonances, too, but the field does not cross zero. In this case, integration of the Berry connection gives the adiabatic Berry phase 2π and the AA phase varies from 0 to (integer multiple of) $\pm 2\pi$ when selecting off-resonance frequencies, similar as in Fig. 2(a).

The adiabatic Berry phase π for the 1:1 bicircular field can be understood as follows. When the field passes zero, its direction suddenly reverses, while the aligned orbital must evolve continuously. After one cycle with three zero crossings, the field returns to its initial direction, whereas, relative to the field, the antisymmetric p orbital has reversed 3 times and thus gained the phase 3π. Hence, passage through the degeneracy offers control of the geometric phase. Figure 3(d) illustrates this for an example (see also the Supplemental Material [68], movie). Here, the p orbital gains a Berry phase of about 0.8π within one period. Because of nonadiabaticity, this value is not exactly π. More generally, a 1:1 bicircular field with frequencies ω and $(N-1)\omega$ has N zero crossings [28], implying an adiabatic Berry phase of $N\pi$.

Spin-1/2 particle in a magnetic field.—Since AA and Berry phases may differ in the adiabatic limit for a circuit that crosses a degeneracy, it is important to reexamine AA's example [21] of a spin-1/2 particle in a magnetic field with a zero crossing. AA assumed a well-defined adiabatic limit for their phase. The Hamiltonian is $H(t) = \mathbf{B} \cdot \boldsymbol{\sigma}/2$ with the Pauli vector $\boldsymbol{\sigma}$. The time-varying magnetic field reads

$$\mathbf{B}(t) = B_0\hat{\mathbf{e}}_z + B_0[\cos(\omega_B t)\hat{\mathbf{e}}_z + \sin(\omega_B t)\hat{\mathbf{e}}_x]. \quad (5)$$

An aligned spin following the field direction cannot suddenly reverse when the field passes zero (degeneracy of the eigenstates), see Fig. 4(a). Thus, the system is expected to return to the initial state only after two rotations of the field [21]. We therefore choose the Floquet frequency $\omega = \omega_B/2$. For both instantaneous eigenstates $[\cos(\omega t/2), \sin(\omega t/2)]^\mathsf{T}$ and $[-\sin(\omega t/2), \cos(\omega t/2)]^\mathsf{T}$, integration of the Berry connection yields π.

The adiabaticity indicator $\mathcal{F}$ for the Floquet states, presented as a function of $\mathcal{N}_B = B_0/\omega_B$ in Fig. 4(b), is

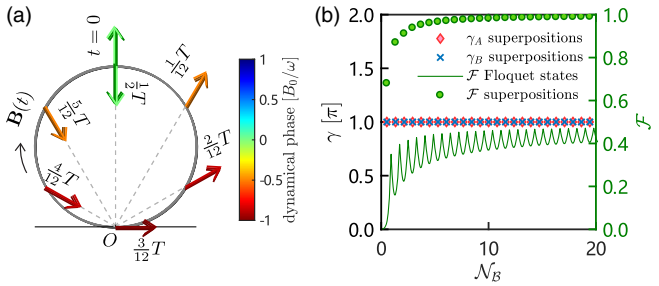

FIG. 4. (a) Illustration of the spin-1/2 state during one rotation of the magnetic field in the limit $\omega \to 0$. Thick arrows indicate the spin direction. The colors represent the dynamical phase. See also the Supplemental Material [68], movie. (b) AA phase γ_A and Berry phase γ_B for the superpositions; adiabaticity indicator $\mathcal{F}$ for Floquet states and superpositions.

below 0.5, i.e., the Floquet states differ strongly from the adiabatic states. Yet, we find that at certain discrete frequencies, the two Floquet states have the same quasienergy and one can superpose them with equal weights such that the superpositions have $\mathcal{F} \approx 1$, i.e., their time evolution is nearly adiabatic [Fig. 4(b)]. For the superpositions, we obtain the geometric phases $\gamma_A = \gamma_B = \pi$, surprisingly without any frequency dependence, see Fig. 4(b). This confirms AA's conclusion. Moreover, we can explain that $\gamma_A = \gamma_B$ arises in this special example because the two energies used for the dynamical phase by Berry and AA are equal: $\bar{\mathcal{E}} = \bar{H} = 0$ due to the antisymmetry of the spin dynamics about the degeneracy. The accumulated dynamical phase after one period is always zero, see Fig. 4(a), which is significant for the implementation of geometric quantum gates.

Conclusion.—Our evaluation of geometric phases for cyclic states passing through a degeneracy reveals both surprises and benefits. Although the Aharonov-Anandan phase often agrees with the adiabatic Berry phase at low frequencies, we have presented a counterexample where they differ although the time evolution is evidently adiabatic. The discrepancy arises because the two definitions employ energies that approach the same low-frequency limit with different speeds. We confirm that the Berry phase affects the low-frequency quasienergies, i.e., observable properties of driven systems. In view of applications in quantum information [17,18] or coherent control of quantum states [69,70], it is of interest that our study suggests convenient control of geometric phases by steering a system through degeneracies.

This work was supported by the National Key Research and Development Program of China under Grant No. 2019YFA0308300, the Deutsche Forschungsgemeinschaft, the National Natural Science Foundation of China under Grants No. 11774109, No. 12174134, No. 12021004, and No. 11627809, and the Alexander von Humboldt Foundation.

*lupeixiang@hust.edu.cn
†lein@itp.uni-hannover.de

[1] M. V. Berry, Quantal phase factors accompanying adiabatic changes, Proc. R. Soc. A **392**, 45 (1984).
[2] H. von Busch, Vas Dev, H.-A. Eckel, S. Kasahara, J. Wang, W. Demtröder, P. Sebald, and W. Meyer, Unambiguous Proof for Berry's Phase in the Sodium Trimer: Analysis of the Transition $A^2E'' \leftarrow X^2E'$, Phys. Rev. Lett. **81**, 4584 (1998).
[3] S. K. Min, A. Abedi, K. S. Kim, and E. K. U. Gross, Is the Molecular Berry Phase an Artifact of the Born-Oppenheimer Approximation?, Phys. Rev. Lett. **113**, 263004 (2014).
[4] F. Bouakline, Unambiguous signature of the Berry phase in intense laser dissociation of diatomic molecules, J. Phys. Chem. Lett. **9**, 2271 (2018).
[5] F. Bernardini, V. Fiorentini, and D. Vanderbilt, Accurate calculation of polarization-related quantities in semiconductors, Phys. Rev. B **63**, 193201 (2001).
[6] F. D. M. Haldane, Berry Curvature on the Fermi Surface: Anomalous Hall Effect as a Topological Fermi-Liquid Property, Phys. Rev. Lett. **93**, 206602 (2004).
[7] L. Fu, C. L. Kane, and E. J. Mele, Topological Insulators in Three Dimensions, Phys. Rev. Lett. **98**, 106803 (2007).
[8] D. Xiao, M.-C. Chang, and Q. Niu, Berry phase effects on electronic properties, Rev. Mod. Phys. **82**, 1959 (2010).
[9] Y.-J. Lin, R. L. Compton, K. Jiménez-García, J. V. Porto, and I. B. Spielman, Synthetic magnetic fields for ultracold neutral atoms, Nature (London) **462**, 628 (2009).
[10] J. Dalibard, F. Gerbier, G. Juzeliūnas, and P. Öhberg, Colloquium: Artificial gauge potentials for neutral atoms, Rev. Mod. Phys. **83**, 1523 (2011).
[11] A. Tomita and R. Y. Chiao, Observation of Berry's Topological Phase by Use of an Optical Fiber, Phys. Rev. Lett. **57**, 937 (1986).
[12] H. Liu, Y. Li, Y. S. You, S. Ghimire, T. F. Heinz, and D. A. Reis, High-harmonic generation from an atomically thin semiconductor, Nat. Phys. **13**, 262 (2017).
[13] A. Chacón, D. Kim, W. Zhu, S. P. Kelly, A. Dauphin, E. Pisanty, A. S. Maxwell, A. Picón, M. F. Ciappina, D. E. Kim, C. Ticknor, A. Saxena, and M. Lewenstein, Circular dichroism in higher-order harmonic generation: Heralding topological phases and transitions in Chern insulators, Phys. Rev. B **102**, 134115 (2020).
[14] R. E. F. Silva, Á. Jiménez-Galán, B. Amorim, O. Smirnova, and M. Ivanov, Topological strong-field physics on sub-laser-cycle timescale, Nat. Photonics **13**, 849 (2019).
[15] G. Hu, X. Hong, K. Wang, J. Wu, H. X. Xu, W. Zhao, W. Liu, S. Zhang, F. Garcia-Vidal, B. Wang, P. Lu, and C. W. Qiu, Coherent steering of nonlinear chiral valley photons with a synthetic Au-WS_2 metasurface, Nat. Photonics **13**, 467 (2019).
[16] J.-S. Xu, K. Sun, J. K. Pachos, Y.-J. Han, C.-F. Li, and G.-C. Guo, Photonic implementation of Majorana-based Berry phases, Sci. Adv. **4**, eaat6533 (2018).
[17] A. Ekert, M. Ericsson, P. Hayden, H. Inamori, J. A. Jones, D. K. L. Oi, and V. Vedral, Geometric quantum computation, J. Mod. Opt. **47**, 2501 (2000).
[18] E. Sjöqvist, Geometric phases in quantum information, Int. J. Quantum Chem. **115**, 1311 (2015).
[19] S. Appelt, G. Wäckerle, and M. Mehring, Deviation from Berry's Adiabatic Geometric Phase in a Xe 131 Nuclear Gyroscope, Phys. Rev. Lett. **72**, 3921 (1994).
[20] Wang Xiang-Bin and Matsumoto Keiji, Nonadiabatic Conditional Geometric Phase Shift with NMR, Phys. Rev. Lett. **87**, 097901 (2001).
[21] Y. Aharonov and J. Anandan, Phase Change during a Cyclic Quantum Evolution, Phys. Rev. Lett. **58**, 1593 (1987).
[22] Z. Wu and J. Wang, Berry's phase and Aharonov-Anandan's phase, Physica A **232**, 201 (1996).
[23] D. B. Milošević, W. Becker, and R. Kopold, Generation of circularly polarized high-order harmonics by two-color coplanar field mixing, Phys. Rev. A **61**, 063403 (2000).
[24] A. Fleischer, O. Kfir, T. Diskin, P. Sidorenko, and O. Cohen, Spin angular momentum and tunable polarization in high-harmonic generation, Nat. Photonics **8**, 543 (2014).

[25] L. Medišauskas, J. Wragg, H. van der Hart, and M. Y. Ivanov, Generating Isolated Elliptically Polarized Attosecond Pulses Using Bichromatic Counterrotating Circularly Polarized Laser Fields, Phys. Rev. Lett. **115**, 153001 (2015).
[26] D. M. Reich and L. B. Madsen, Illuminating Molecular Symmetries with Bicircular High-Order-Harmonic Generation, Phys. Rev. Lett. **117**, 133902 (2016).
[27] D. Baykusheva, S. Brennecke, M. Lein, and H. J. Wörner, Signatures of Electronic Structure in Bicircular High-Harmonic Spectroscopy, Phys. Rev. Lett. **119**, 203201 (2017).
[28] A. D. Bandrauk, J. Guo, and K.-J. Yuan, Circularly polarized attosecond pulse generation and applications to ultrafast magnetism, J. Opt. **19**, 124016 (2017).
[29] Á. Jiménez-Galán, N. Zhavoronkov, D. Ayuso, F. Morales, S. Patchkovskii, M. Schloz, E. Pisanty, O. Smirnova, and M. Ivanov, Control of attosecond light polarization in two-color bicircular fields, Phys. Rev. A **97**, 023409 (2018).
[30] O. Neufeld, D. Podolsky, and O. Cohen, Floquet group theory and its application to selection rules in harmonic generation, Nat. Commun. **10**, 405 (2019).
[31] S. Odžak, E. Hasović, and D. B. Milošević, High-order harmonic generation in polyatomic molecules induced by a bicircular laser field, Phys. Rev. A **94**, 033419 (2016).
[32] S. Eckart, K. Fehre, N. Eicke, A. Hartung, J. Rist, D. Trabert, N. Strenger, A. Pier, L. P. H. Schmidt, T. Jahnke, M. S. Schöffler, M. Lein, M. Kunitski, and R. Dörner, Direct Experimental Access to the Nonadiabatic Initial Momentum Offset upon Tunnel Ionization, Phys. Rev. Lett. **121**, 163202 (2018).
[33] D. J. Moore and G. E. Stedman, Non-adiabatic Berry phase for periodic Hamiltonians, J. Phys. A **23**, 2049 (1990).
[34] D. J. Moore, The calculation of nonadiabatic Berry phases, Phys. Rep. **210**, 1 (1991).
[35] J. Liu, B. Hu, and B. Li, Nonadiabatic Geometric Phase and Hannay Angle: A Squeezed State Approach, Phys. Rev. Lett. **81**, 1749 (1998).
[36] References [33,34] use the term "non-adiabatic Berry phase" for the AA phase. We reserve the term "Berry phase" for values obtained with Berry's definition of the dynamical phase.
[37] J. H. Shirley, Solution of the Schrödinger equation with a Hamiltonian periodic in time, Phys. Rev. **138**, B979 (1965).
[38] C. J. Joachain, N. J. Kylstra, and R. M. Potvliege, *Atoms in Intense Laser Fields* (Cambridge university Press, New York, 2012), pp. 141–158.
[39] L. Medišauskas, U. Saalmann, and J. M. Rost, Floquet Hamiltonian approach for dynamics in short and intense laser pulses, J. Phys. B **52**, 015602 (2019).
[40] R. Moessner and S. L. Sondhi, Equilibration and order in quantum Floquet matter, Nat. Phys. **13**, 424 (2017).
[41] H. Hübener, M. A. Sentef, U. De Giovannini, A. F. Kemper, and A. Rubio, Creating stable Floquet-Weyl semimetals by laser-driving of 3D Dirac materials, Nat. Commun. **8**, 13940 (2017).
[42] T. Oka and H. Aoki, Photovoltaic Hall effect in graphene, Phys. Rev. B **79**, 081406(R) (2009).
[43] Y. H. Wang, H. Steinberg, P. Jarillo-Herrero, and N. Gedik, Observation of Floquet-Bloch states on the surface of a topological insulator, Science **342**, 453 (2013).
[44] We use atomic units throughout this Letter.
[45] A. Russomanno, S. Pugnetti, V. Brosco, and R. Fazio, Floquet theory of Cooper pair pumping, Phys. Rev. B **83**, 214508 (2011).
[46] L. Li, P. Lan, L. He, X. Zhu, J. Chen, and P. Lu, Scaling Law of High Harmonic Generation in the Framework of Photon Channels, Phys. Rev. Lett. **120**, 223203 (2018).
[47] M. Pont, R. Shakeshaft, and R. M. Potvliege, Low-frequency theory of multiphoton ionization, Phys. Rev. A **42**, 6969 (1990).
[48] M. Pont, R. M. Potvliege, R. Shakeshaft, and Z.-j. Teng, Low-frequency theory of multiphoton ionization. II. General formulation and further results for ionization of H(1s), Phys. Rev. A **45**, 8235 (1992).
[49] H. Martiskainen and N. Moiseyev, Perturbation theory for quasienergy floquet solutions in the low-frequency regime of the oscillating electric field, Phys. Rev. A **91**, 023416 (2015).
[50] H. Martiskainen and N. Moiseyev, Adiabatic perturbation theory for atoms and molecules in the low-frequency regime, J. Chem. Phys. **147**, 224101 (2017).
[51] A. Russomanno and G. E. Santoro, Floquet resonances close to the adiabatic limit and the effect of dissipation, J. Stat. Mech. (2017) 103104.
[52] M. Rodriguez-Vega, M. Lentz, and B. Seradjeh, Floquet perturbation theory: Formalism and application to low-frequency limit, New J. Phys. **20**, 093022 (2018).
[53] M. Lein, E. K. U. Gross, and V. Engel, Discrete peaks in above-threshold double-ionization spectra, Phys. Rev. A **64**, 023406 (2001).
[54] M. Born and V. Fock, Beweis des Adiabatensatzes, Z. Phys. **51**, 165 (1928).
[55] D. M. Tong, K. Singh, L. C. Kwek, and C. H. Oh, Sufficiency Criterion for the Validity of the Adiabatic Approximation, Phys. Rev. Lett. **98**, 150402 (2007).
[56] M. H. S. Amin, Consistency of the Adiabatic Theorem, Phys. Rev. Lett. **102**, 220401 (2009).
[57] N. Bleistein, Uniform asymptotic expansions of integrals with stationary point near algebraic singularity, Commun. Pure Appl. Math. **19**, 353 (1966).
[58] M. Lewenstein, Ph. Balcou, M. Yu. Ivanov, Anne L'Huillier, and P. B. Corkum, Theory of high-harmonic generation by low-frequency laser fields, Phys. Rev. A **49**, 2117 (1994).
[59] S. Eckart, M. Kunitski, M. Richter, A. Hartung, J. Rist, F. Trinter, K. Fehre, N. Schlott, K. Henrichs, L. Ph. H. Schmidt, T. Jahnke, M. Schöffler, K. Liu, I. Barth, J. Kaushal, F. Morales, M. Ivanov, O. Smirnova, and R. Dörner, Ultrafast preparation and detection of ring currents in single atoms, Nat. Phys. **14**, 701 (2018).
[60] T. Herath, L. Yan, S. K. Lee, and W. Li, Strong-Field Ionization Rate Depends on the Sign of the Magnetic Quantum Number, Phys. Rev. Lett. **109**, 043004 (2012).
[61] X. M. Tong and C. D. Lin, Empirical formula for static field ionization rates of atoms and molecules by lasers in the barrier-suppression regime, J. Phys. B **38**, 2593 (2005).
[62] I. Barth and M. Lein, Numerical verification of the theory of nonadiabatic tunnel ionization in strong circularly polarized laser fields, J. Phys. B **47**, 204016 (2014).

[63] X. Zhang, L. Li, X. Zhu, K. Liu, X. Liu, D. Wang, P. Lan, I. Barth, and P. Lu, Subpetahertz helicity-modulated high-order harmonic radiation, Phys. Rev. A **98**, 023418 (2018).

[64] K. Liu, H. Ni, K. Renziehausen, J. M. Rost, and I. Barth, Deformation of Atomic $p_{\pm}$ Orbitals in Strong Elliptically Polarized Laser Fields: Ionization Time Drifts and Spatial Photoelectron Separation, Phys. Rev. Lett. **121**, 203201 (2018).

[65] J. W. Zwanziger and E. R. Grant, Topological phase in molecular bound states: Application to the $E \otimes e$ system, J. Chem. Phys. **87**, 2954 (1987).

[66] Very small $\mathcal{N}$ are excluded from Figs. 2, 3 because of avoided crossings between s and p states that we do not discuss in the present work.

[67] R. Requist, F. Tandetzky, and E. K. U. Gross, Molecular geometric phase from the exact electron-nuclear factorization, Phys. Rev. A **93**, 042108 (2016).

[68] See Supplemental Material at http://link.aps.org/supplemental/10.1103/PhysRevLett.128.030401 for animated versions of Figs. 3(d) and 4(a).

[69] F. Vewinger, M. Heinz, B. W. Shore, and K. Bergmann, Amplitude and phase control of a coherent superposition of degenerate states. I. Theory, Phys. Rev. A **75**, 043406 (2007).

[70] A. Karpati and Z. Kis, Adiabatic creation of coherent superposition states via multiple intermediate states, J. Phys. B **36**, 905 (2003).